The Correlation of Chemical Structure to Tribological Properties of Polyimide Thin Films

by

John W. Jones

Thesis submitted to the Faculty of the
Virginia Polytechnic Institute and State University
in partial fulfillments of the requirements for the degree of

MASTER OF SCIENCE

in

Mechanical Engineering

Approved:

N. S. Eiss, Jr., Chairman

H. H. Mabie

D. W. Dwight

May 1983

Blacksburg, Virginia

THE CORRELATION OF CHEMICAL STRUCTURE TO TRIBOLOGICAL PROPERTIES OF POLYIMIDE THIN FILMS

by

John Walter Jones

(ABSTRACT)

The friction and wear behavior of three thin polyimide films of known chemical structure was tested. An attempt was made to correlate differences in chemical structure, primarily the presence of flexible linkages and highly polar side groups, to differences in tribological properties. The wear test results showed lowest wear for the polyimide with the flexible oxygen linkage. The wear mechanism was deduced to be fatigue since wear did not occur immediately and a strong correlation was noted between wear rate and elastic modulus. Increasing sliding speed increased both wear rate and friction coefficient. The friction results showed highest friction for the polyimide with the highest density of polar side groups. Even though some effects of the deformation component of friction were seen, the adhesive component of friction predominated.

ACKNOWLEDGEMENTS

The author is indebted to Dr. N. S. Eiss, Jr. for his valuable assistance throughout the course of this research. His advice and guidance are sincerely appreciated.

Dr. H. H. Mabie and Dr. D. W. Dwight are thanked for their service on the graduate committee. Special thanks go to and for their assistance in the film spreading and curing operations. is thanked for the use of his lab equipment. and gave much advice concerning the chemical aspects of this research. is thanked for sharing his polyimide thin film experience. The suggestions of are especially appreciated. is thanked for supplying the polymer solutions.

The author would also like to thank his parents for their encouragement throughout his college career.

TABLE OF CONTENTS

LIST OF TABLES

LIST OF FIGURES

INTRODUCTION

Polyimides are long chain molecules which have recurring imide groups as an integral part of their main chain. The characteristic imide linkage is shown in Fig. 1 [1]*.

High thermal stability is especially characteristic of aromatic polyimides, which are polyimides derived from aromatic diamines and hence contain aromatic groups in their backbone.

The major portion of research on the tribological properties of polyimides has been done by R. L. Fusaro. In testing performed on thin polyimide films, Fusaro found that polyimides wear by an adhesive wear mechanism at a linear rate [2]. In an inert atmosphere, wear is reduced by an order of magnitude [3]. Fusaro found that the polyimides he tested could be divided into two groups according to friction and wear properties. Group I polyimides generally have lower friction and higher wear than group II polyimides. Fusaro's results suggested that a linear non-crosslinked polyimide will have a higher wear rate than a polyimide characterized by some crosslinking [2]. Fusaro has also noted that polyimides undergo a transition from high friction, high wear to low friction, low wear as the temperature is increased above about 40°C. No correlation between this transition and a molecular relaxation was found [4]. In much of the previous research into polyimide tribology,

---

*Numbers in brackets refer to references at the end of the thesis.

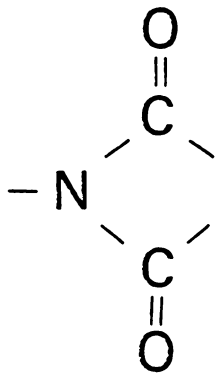

Figure 1: Characteristic Imide Linkage

polyimides whose chemical structure is proprietary were tested. Consequently, generalizations about structure-property relationships have been hindered.

In previous research performed at VPI&SU Potter attempted to observe the formation of an abrasively formed wear particle in the scanning electron microscope (SEM). He noted that even for polymer contacting with sharp asperities the polymer tended to flow around the asperities and that cumulative damage developed due to the low level contact stresses. In experiments of a steel sphere sliding on polymer disks, he noted an initial period of no measurable wear (or incubation period) followed by the sudden formation of a wear track. These observations led to interest in using a fatigue model to describe polymer wear.

Carter [5] investigated the wear and friction of polyethyleneterephthalate using a constant strain wear test apparatus. He found that the polymer fatigued at the surface, due to irregularities, inhomogeneities, and localized adhesive forces, rather than below the surface where the distortion energy was highest. He also noted an increase in adhesive force as the number of cycles of the test increased.

In this research friction and wear testing on polyimides of known chemical structure is presented. In all tests, a steel ball was loaded against a thin (approximately 50μm thick) rotating polyimide film cast on a stainless steel substrate.

In following sections of this paper, a review of polyimide and polyimide friction and wear literature will be presented, followed by

the experimental procedure and results. Then, an attempt will be made to explain the relative tribological performance of each polyimide according to its chemical structure.

LITERATURE REVIEW

General Properties

Polyimides are long chain molecules which have recurring imide groups as an integral part of their main chain. Polyimides derived from aliphatic diamines are generally soluble, thermoplastic, and have one step preparation reactions, while aromatic polyimides, which are derived from aromatic diamines, are generally insoluble. Polyimides are generally amorphous, however up to 50 per cent crystallinity can be induced in some polyimides. Aromatic polyimides form high molecular weight units only through the use of highly polar solvents, which prevent the reactants from solidifying [6]. A representative aromatic polyimide is shown in Fig. 2.

Polyimides are characterized by not only high thermal stability, but also high radiation stability and high resistance to attack by most chemicals and solvents. They can react with strong alkalis.

Polyimides are excellent dielectrics and are widely used as metal coatings and wire insulators. The properties of an aromatic polyimide can vary widely as a function of its structure. Reference 8 contains a table showing the mechanical properties of some aromatic polyimides at 20°C and 400°C. Some mechanical properties of DuPont Vespel, which is an aromatic polyimide, are given in Table 1 [9].

For most high temperature polymers which contain fused rings in the backbone, structure-property relationships are complicated by the fact that these polymers have a complex mixture of "cis" and "trans" isomers. However, polyimides are unique because the imide rings are symmetrical,

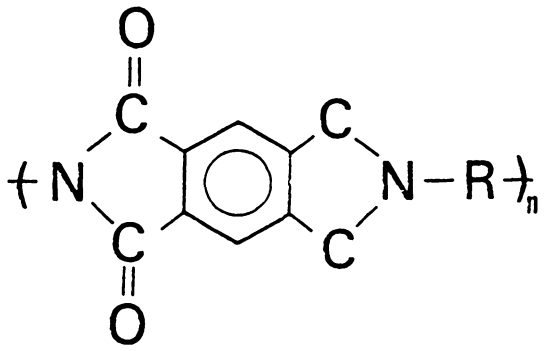

Figure 2: Aromatic Polyimide

Table 1 Some Mechanical Properties of DuPont "Vespel" Aromatic Polyimide

Modulus of Elasticity (GPa)	3.10 at Room Temperature 1.55 at 315°C
Ultimate Tensile Strength (MPa)	75.8
Elongation to Failure	5% for 20 - 250°C
Thermal Expansion Coeff. ($\frac{\mu m}{m}$/C°)	50-63
Water Absorption	
24 hr immersion at 22°C	0.32%
48 hr immersion at 50°C	0.82%

precluding positional isomerism. Despite this, structure-property relations are often obscured by the effects of defects in the molecular structure, thermal prehistory of the polyimide, different chemical reactivities of the precursor acids, and thermal reactions which occur near transition temperature [10]. One general trend that has been noted for polyimides is that the degree of crystallinity increases with the presence of symmetrical diamine and dianhydride groups.

Prokopchuk et. al. [11] tested the mechanical properties of four aromatic polyimides before and after using thermal elongation to induce a degree of crystallinity. They observed a significant increase in strength and modulus of elasticity and a significant decrease in the elongation to failure after the crystallization treatment.

Wallach [12] found that for polyimide films a wide molecular weight distribution favors higher mechanical properties. He noted that mechanical properties, such as tensile strength and elongation to failure, vary with molecular weight average and distribution, intrinsic viscosity and sedimentation constant.

Thermal Stability

Even though aromatic polyimides can have widely varying properties, they are almost all characterized by high temperature stability. The primary factors which contribute to the thermal stability of aromatic polyimides are that the aromatic groups form a more rigid backbone, permit broken bonds to reform, and allow less Brownian motion.

Cassidy and Dekker [13] note three major ways to improve the thermal stability of a polymer: increase crystallinity, increase

crosslinking, or remove thermo-oxidative weak links. Hergenrother [14] lists a number of chemical and physical factors which contribute to thermal stability. The chemical factors include primary bond strength, Van der Waal's bonding forces, hydrogen bonding, and resonance stabilization. The physical factors include high molecular weight, molecular symmetry, rigid intrachain structure, degree of crystallinity, polar groups, and crosslinking.

The factor which often determines thermally stability is the absence of flexible linkages, such as those formed between oxygen or aliphatic groups and the carbon atoms. The introduction of either oxygen or aliphatic groups in either main or side chain will result in poorer stability [15].

The nature of the aromatic groups in the backbone also affects thermal stability. Para-phenylene aromatic groups produce more thermally stable polyimides than meta-phenylene groups, due to the para group's tendency to form more highly ordered, more crystalline, and higher density polymers. There is also a greater probability of a para-phenylene group stabilizing a broken intermolecular chain bond [16].

Molecular Relaxations and Transitions

Most polyimides display a glass transition (T_g) and also at least one sub-T_g transition, (T_B), which is usually called the secondary glass transition. The primary glass transition is associated with large chain segments obtaining enough energy to move relative to one another. The secondary transition is usually associated with torsional oscillations of aromatic groups leading to reorientation of a short segment of a

chain [17]. Lower temperature transitions are also noted for polyimides.

For most aromatic polyimides, the glass transition temperature lies between 550 and 650 K. The secondary transition, which researchers have attempted to correlate with tribological properties, occurs between about 350 and 400 K. Ikeda [18] postulates that for polyimide film this transition, or relaxation, is due to an interplanar slippage mechanism similar to that of graphite. Bernier and Kline [19] noted that the transitions are both temperature and frequency dependent, and found the secondary transition at a temperature near that found by Ikeda. However, since Bernier and Kline found no x-ray evidence of crystallinity in their sample, they doubted Ikeda's interplanar slippage mechanism. Lim et al. [20] also refuted Ikeda's model and theorized that for polyimides the secondary transition is due to combined reorientational movement of rings and connecting atoms in regions of poor chain packing. Butta, DePetris, and Pasquini [17] note that as frequency is increased, the transition occurs at higher temperatures, and that the polyimide modulus of elasticity does not undergo any sharp change at the transitions.

Tribological Properties

The major portion of research on the friction and wear of polyimides has been done by R. L. Fusaro. Fusaro has concentrated his research on polyimide thin films, (25μm thick), using a rider on disk apparatus. Fusaro found that polyimides fall into two groups according to friction and wear properties. Group I polyimides, generally have lower friction and higher wear than group II polyimides. The wear of

both groups, according to Fusaro, occurs by an adhesive wear mechanism, with larger wear particles being formed by group I polyimides [2].

Fusaro has found that polyimides undergo a transition from high friction and high wear to low friction and low wear at about 40°C. This transition was found to be reversible and independent of sliding velocity [4]. Fusaro believes that this friction transition occurs due to some molecular relaxation which gives molecules a degree of freedom so that an external mechanical stress can rearrange the molecules into a structure conductive to shear, i.e. an extended chain. This transformation of folded chains into extended chains can occur in two ways: by plastic deformation, in which the chains simply unfold in the direction of the force, or by shear deformation, in which the chains gradually become tilted by twisting and slipping, and thus become progressively oriented in the direction of the force [4, 21].

Below the transition, polyimides undergo powdery wear, moisture leads to lower wear and lower friction, and no initial period of high friction is noted. Above the transition, wear occurs by a film-like plastic flow, and high initial friction is noted, except in moist air. Moisture is found to have detrimental effects on friction and wear for temperatures between the transition temperature and 200°C, above which no effect was noted [2, 3, 22]. The presence of moisture was thought to constrain molecular orientation of the polyimide chains and also to inhibit adhesion of the polyimide to the rider, which would account for the beneficial effects of moisture on friction and wear [21, 22].

In two sets of experiments, Fusaro has unsuccessfully attempted to correlate the polyimides' tribological transition region to a molecular

relaxation region. The difference between the friction transition temperature and the secondary glass transition temperature was large enough that even considering heat generated by friction in the contact area, no direct correlation was found. However, in the discussion of Reference 23, Kenneth Ludema notes that this lack of correlation between friction transition and molecular relaxations may be due to the different strain rates in the tests. Dr. Ludema also suggests that the molecular orientation postulated by Fusaro should be detectable with diffraction work.

Other tribological information suggested by Fusaro is that the polyimide thin films undergo linear wear rates, and have an order of magnitude longer wear lives in inert atmospheres [3]. Friction increases with time since the polyimide film in the contact zone is gradually depleted by flowing out of the sides of the wear track resulting in an increased metallic contact [24]. Above 300°C, friction is dependent on the thermal prehistory of the polyimides. Pre-heating allows more crosslinking and longer chains, thus inhibiting large scale movements [4].

In one of Fusaro's most recent works, published in February 1980, he compared the tribological properties at 25°C of seven polyimide films bonded to type 301 stainless steel. Brittle fracture and spalling occurred in all films in less than 1000 cycles of sliding. Even though the nominal stress in the film was only about 1250 psi, spalling occurred due to the films' inability to withstand tensile stresses imposed by the local deformations (misalignment, edge effects, and asperity interactions) of the steel substrate. From this, Fusaro infers

that a hard substrate is necessary for good lubrication with polyimide films [25].

Of the seven polyimides tested in this study, Fusaro provides chemical structures for two of them, PIC-6 and PIC-7. PIC-6 has oxygen groups linking some of its aromatic rings while PIC-7 has no oxygen linking groups. PIC-7 has a high density of carbonyl groups. The PIC-7 polyimide underwent much worse spalling and wore away much quicker than the PIC-6 polyimide. This could be predicted from the chemical structures since the PIC-6 backbone contains the flexible oxygen carbon links and consequently should have lower elastic modulus than the more rigid PIC-7 structure [25].

Also in 1980, Fusaro used optical microscopy to investigate the film wear mechanism of polyimide-bonded graphite fluoride. He observed two wear mechanisms: one in which the film plastically flowed and tended to disengage by spalling, and another in which entire chunks of the film disengaged by cracks propagating through defects in the bulk [26].

Giltrow [27], who used a cylinder on cylinder apparatus, observed no evidence of Fusaro's friction and wear transition and instead noted a smooth parabola-like decline in friction coefficient from 20°C to about 220°C. Above 220°C he observed a gradual rise in friction. The mechanism of lubrication was by transfer films which reduced the effective counterface surface roughness.

Salomon [28] notes that friction transitions have been detected in polytetrafluoroethylene (PTFE) and high density polyethylene (HDPE). He theories that the wear of polyimides takes place through a large scale

transfer mechanism in which polyimide elements are transferred from film to pin before they leave the system as wear debris. For high damping, which corresponds to internal softening, larger volume elements are transferred. For temperatures under about 50°C, the polyimide molecular groups are capable of only short range movements, leading to impact toughness which partially counterbalances the effect of higher friction on wear life. For temperatures about 50°C, long range motions of molecular chains are possible, enabling sufficient flow and transfer to form strongly coherent surface layers on both surfaces. This layered configuration leads to lower friction and lower wear. Above 400°C, the effect of creep predominates, leading to higher wear.

Bill [29] tested polyimide coatings as a possible means to prevent fretting of steel. He noted that the polyimide coating reduced wear to the uncoated surface only marginally. The wear of the polyimide coating was high and attributed to an abrasive wear mechanism.

Buckley and Johnson [30] used a polyimide pin on stainless steel disk apparatus in vacuum. They found low wear and low friction for polyimide on steel and higher friction and extremely low wear for polyimide on polyimide.

Buckley [31] used a polyimide pin on disks of four different materials, a tool steel, a stainless steel, copper, and stellite 6B, to determine the effect of substrate on polyimide friction and wear. A change in substrate was found to have little effect on wear. Friction differences were noted but could not be correlated to substrate hardness. Since all tests exhibited a running-in period, Buckley postulated that lubrication resulted from the formation of a transfer film and that

the friction forces were consequently the sum of two components: the friction of the polyimide on the transfer film and the friction of the polyimide on the metal. He further stated that friction differences for polyimides on different substrates may be due to the type of transfer film formed, in particular its continuity and the degree of metal to polyimide contact through it.

Kroll and Devine [32] tested polyimide retaining rings in ball bearings and found low friction but low service lives due to retaining ring failure. In close tolerance applications fracture of polyimide components may occur due to thermal expansion.

Gardos [33] tested polyimides as binding agents for self-lubricating composites. He found that thermosetting polyimides gave better wear performance at high temperatures than did a non-thermosetting polyimides (with a Tg = 370°C). The non-thermosetting polyimide performed as well as the thermosetting polyimides at room temperature, but tended to crumble at the test temperature of 316°C.

Jones, Hady, and Johnson [34] tested the friction and wear of a polyimide, a poly(amid-imide), and a pyrrone at 260°C in dry air. They found friction coefficients to be less than 0.20 and nearly equal for all three. The pyrrone exhibited relatively low wear, the polyimide, intermediate wear, and the poly(amid-imide) high wear.

Prikhodko et. al. [35] performed research on heat resistant aromatic polyamides and found lower abrasion resistance and higher friction for crystalline polyamides than amorphous polyamides.

Summary

In summary it is observed that there is not a great deal of agreement in the research performed on polyimide friction and wear. It is generally agreed that for polyimide on steel, friction decreases from about 20°C to 220°C and then increases slightly for higher temperatures. A point of contention is the nature of the decrease from 20°C to 220°C. Fusaro [2] notes a sharp decrease at about 40°C, while Giltrow [27] notes a steady decline.

The mechanisms of wear and lubrication are also not agreed upon. Fusaro has noted an adhesive wear mechanism [2], a spalling wear mechanism [26], and a wear mechanism in which the polyimide plastically flows out of the contact area [24]. Salomon and DeGee [28] observed large-scale transfer of polyimide to steel as a wear mechanism. Giltrow [27] noted this formation of a transfer film as a lubrication mechanism. Buckley [31] also noted the formation of a transfer film. In the research of Kroll and Devine [32] wear occurred due to fracture of the polyimide. Bill [29] observed an abrasive wear mechanism in his study of using polyimide coatings to prevent fretting wear.

Finally, it is noted that there are many areas in need of further research:

1) the verification of Fusaro's friction and wear transition temperature.
2) the correlation of the tribological transition with some molecular transition.

3) the characterization of the mechanisms of polyimide wear and lubrication, perhaps using surface analysis techniques.

4) the effect of crystallinity on tribological properties, using a technique similar to that of Prokopchuk et. al. [11].

5) the effect of the diamine or dianhydride on tribological properties.

EXPERIMENTAL PROGRAM

Film Preparation

Polyamic acid solutions, obtained from NASA in Langley, Virginia, were spread onto stainless steel substrates and cured to produce thin polyimide films. Details of the casting and curing procedure are presented in Appendix A. The polyimides were polymerized from dianhydride and diamines which differed by only a linking group. The structures of the resultant polyimides, which were arbitrarily named "PIA, PIB, and PIC", are shown in Fig. 3.

The curing procedure tightly adhered the films to the substrate and, by driving off solvent, reduced the film thickness to about 50μm. The actual film thicknesses and a measure of their consistency is shown in Table 2. The polyimide film mechanical properties are given in Appendix B. The films were stored in a dessicator with anhydrous calcium chloride when not being tested.

Friction and Wear Testing

All friction and wear testing was performed using the pin-on-disk wear machine shown in Fig. 4. A 3.17mm diameter steel ball was loaded, using a pneumatic device, against the polyimide film being rotated by a motor. Before each test, the ball and film were cleaned with acetone. With the exception of the double speed tests, the linear velocity of the substrate relative to the ball was held constant at 0.628 meters per second. In all tests, the ambient temperature was approximately 22°C and the relative humidity approximately 40 per cent.

		η_{inh},* dl/g	T_g,**°C
PIA	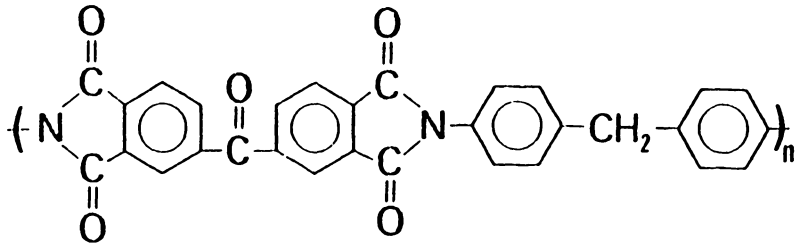	1.30	295
PIB	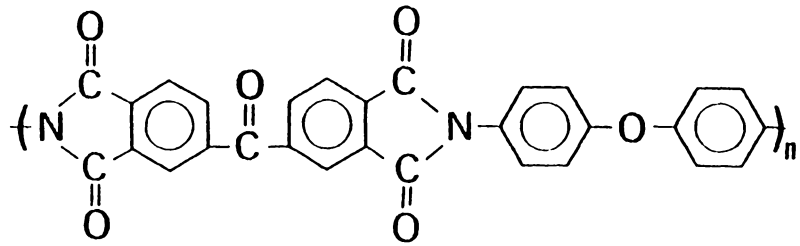	1.49	257
PIC	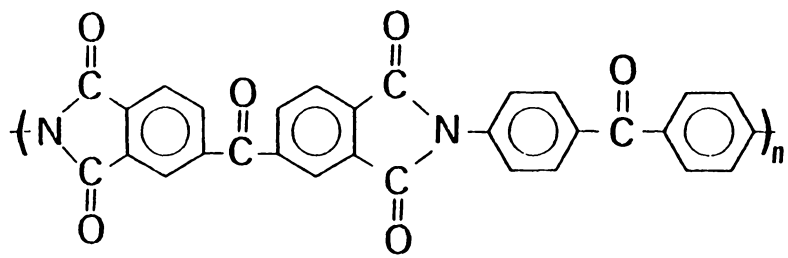	0.91	288

* Inherent viscosity in deciliters per gram of polyamic acid at 25°C.
** Glass transition temperature of polyimide film dried through 200°C for one hour, thermal mechanical analysis at heating rate of 5°C per minute.

Figure 3: Chemical Structure and Properties of Tested Polyimides

Table 2 Film Thickness After Curing

	Film Thickness (mm)	Standard Deviation (mm)
PIA	0.0625	0.0028
PIB	0.0528	0.0003
PIC	0.0396	0.0030

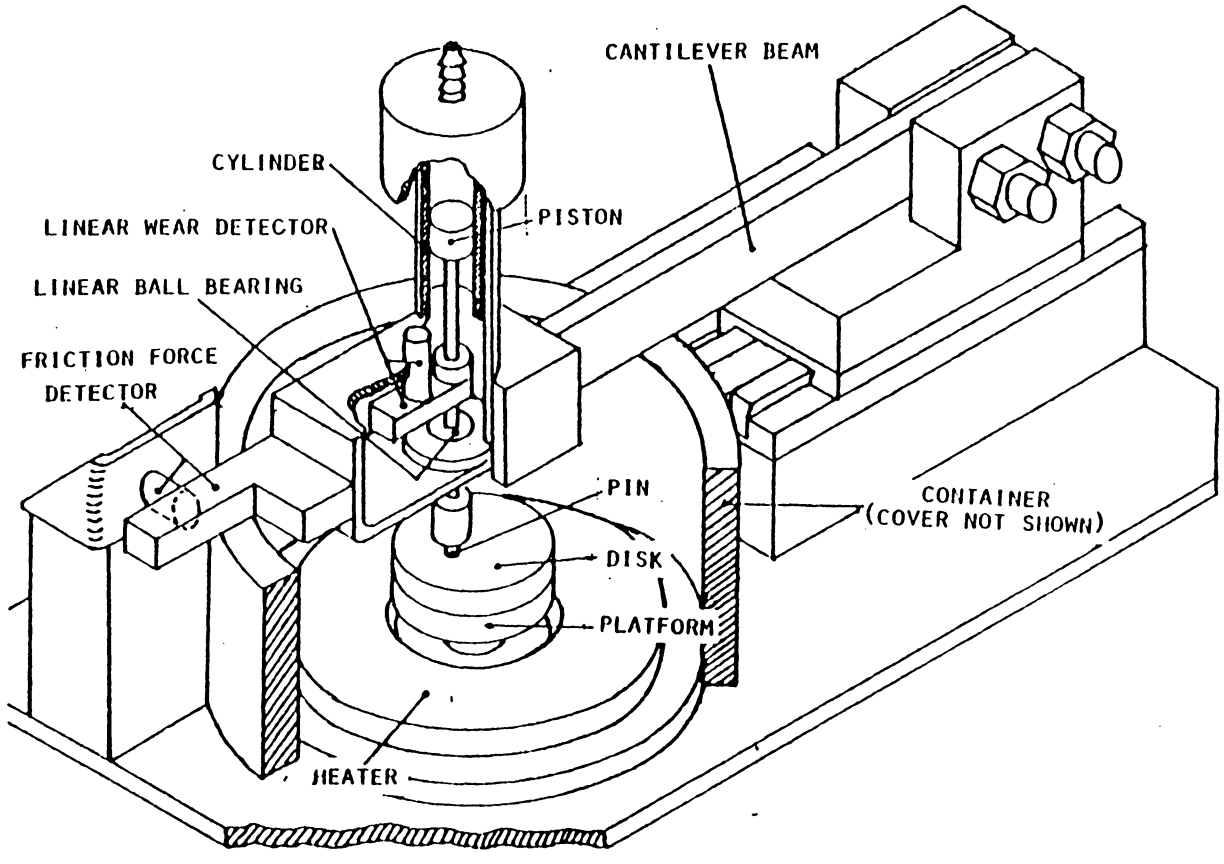

Figure 4: Pin-on-Disk Wear Machine [36]

Friction

Friction forces caused a deflection, measured by a proximity transducer, of the cantilever beam to which the ball was attached. The output of the proximity transducer was recorded on an X-Y plotter, yielding a continuous measure of the friction force. The friction measurement system was calibrated before and at least once during the test.

Friction tests were conducted at loads of 5 and 10 N. During most testing, the initiation of a wear track was accompanied by a sharp increase in the friction force. The representative friction plot seen in Figure 5 shows these effects. In friction analysis, the friction just after initiation was defined as the friction force value when the friction force resumes its normal variation per revolution. For purposes of comparison, the friction coefficient was calculated just after the initiation of a wear track (usually less than 1000 cycles) μ_{after}, after 2000 cycles μ_{2000}, and after 16000 μ_{16000} cycles. The complete experimental conditions for the friction testing are presented in Table 3.

Wear

Preliminary testing was conducted at loads of 2, 3, 5, 7.5, and 10 N to determine which load most conveniently exhibited the difference in the polyimides' wear performance. At loads of 2 and 3 N, incubation periods were relatively long and widely varying. The 5 N load was

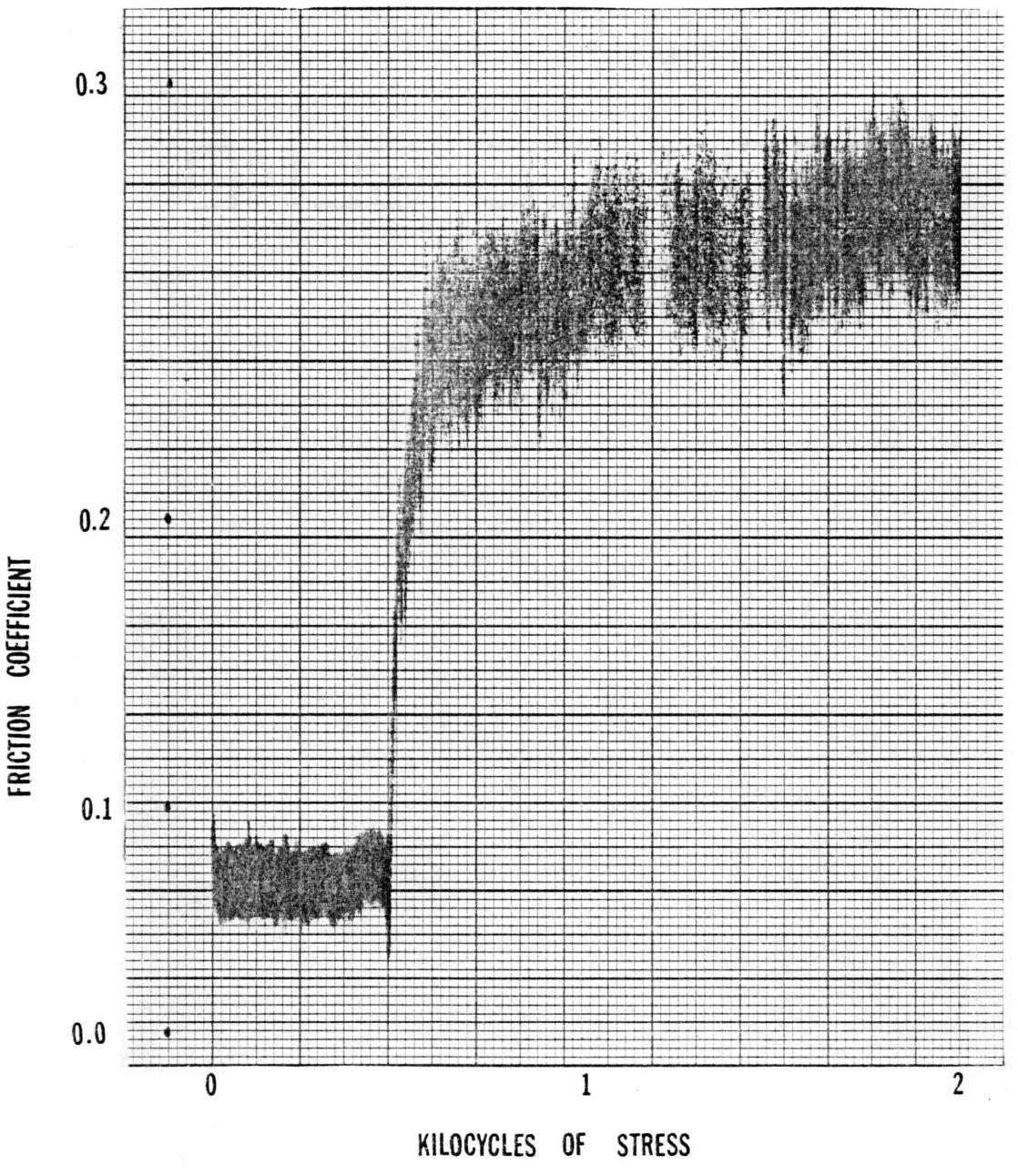

Figure 5: Representative Friction Force Plot

Table 3 Experimental Conditions for Friction Testing

Number of tests performed under each set of conditions

Temperature = 22°C Relative Humidity = 40 per cent

		μ_{after}	μ_{2000}	μ_{16000}
Speed = 0.63 $\frac{m}{s}$ Load = 5 N	PIA	7	7	4
	PIB	--	10	4
	PIC	10	7	4
Speed = 0.63 $\frac{m}{s}$ Load = 10 N	PIA	5	6	0
	PIB	--	5	0
	PIC	6	6	0
Speed = 1.26 $\frac{m}{s}$ Load = 5 N	PIC	3	3	3

chosen because it best illustrated the wear performance of the polyimides and evoked a more elastic state of stress than the higher loads. The complete wear test conditions are presented in Table 4.

The wear of the polyimide film was measured by stopping the tests at intervals of 2000 cycles and taking four surface profiles, using a Talysurf 4 profilometer, of the wear track. Each profile sampling was taken along a line perpendicular to an edge of the film and passing through the substrate center as shown in Fig. 6. The cross-section area of the wear track was obtained by approximating the area as a trapezoid. For irregularly shaped tracks, which occurred when the surface was slightly sloped, a convention of drawing the top line of the trapezoid parallel to the bottom line was adopted. A representative wear track profile, before and after trapezoidal modeling is shown in Fig. 7. The wear was quantified by taking the average of four cross section areas. Wear rates were obtained by using linear regression on the average cross section areas versus number of cycles plot. The wear values at 2000 cycles were not used in the regression since they do not represent steady state conditions.

Table 4 Wear Test Conditions

Ambient Temperature:	22°C
Relative Humidity:	40 per cent
Load:	5 N
Speed:	0.63 meters per second
Radii of Wear Tracks:	0.94 - 2.93 centimeters

NOTE: PIC was also tested at a speed of 1.26 meters per second.

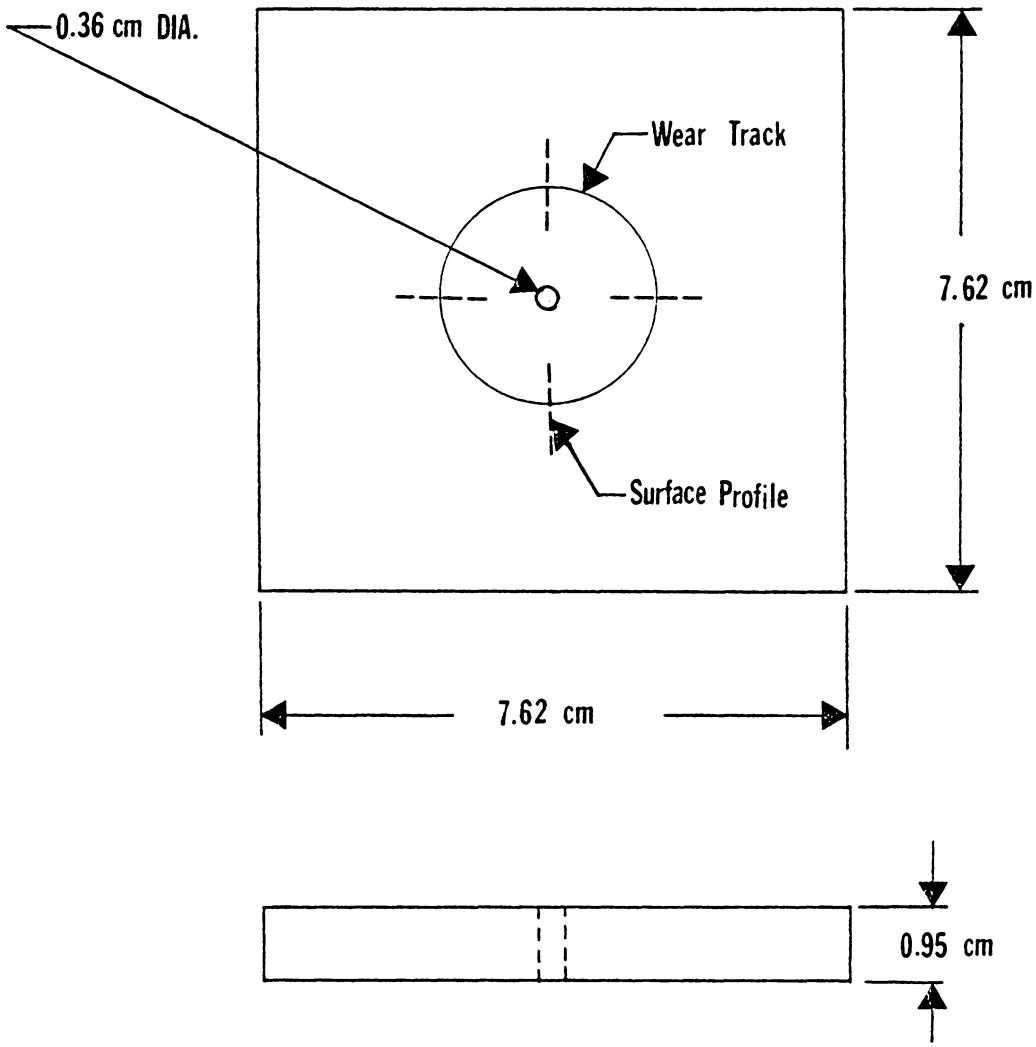

Figure 6: Location of Profile Sampling

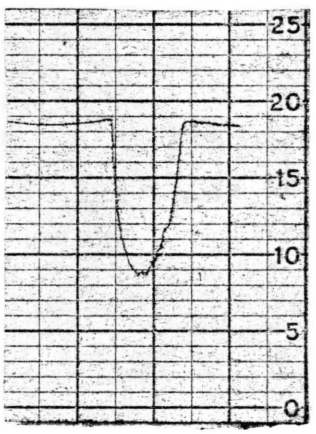

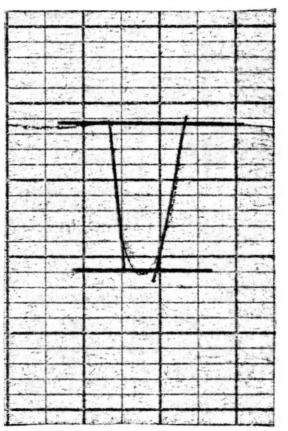

Before trapezoidal modeling

After trapezoidal modeling

1 mm

0.01 mm

Figure 7: Representative Wear Track Profile

RESULTS

A. Wear

The average wear rate and Y-intercept values for the three polyimides are shown in Table 5. PIB had one-third the wear of PIA and PIC. Statistically, the differences in wear rate between PIA and PIC were not significant enough to assert the conclusion of different wear performance for PIC. Fig. 8 shows the average wear, as measured by the average cross-sectional area of the wear track, versus the number of cycles. In a typical wear test, the polyimide film underwent an initial period of no wear followed by the rapid initiation of a wear track followed by approximately linear wear. The random nature of the wear track initiation is illustrated by Table 6. At a load of 5 N, wear occurred first on PIC, followed by PIA, followed by PIB. At a load of 10 N, wear occurred sooner on PIB than on PIA, although the results were variable. Increasing the load decreased the incubation period for PIB and PIC, yet increased the incubation period for PIA. For PIC, the effect of doubling the speed was to increase the incubation period. No correlation of the wear track initiation to heat build-up at the sliding interface was found.

For PIC, doubling the sliding speed increased the wear rate (per cycle) by 37 per cent, as shown in Table 7. Fig. 9 shows the wear rates for PIC at sliding speeds of 0.63 meters per second and 1.26 meters per second. Complete wear test data is presented in Appendix C.

Table 5 Wear Rates and Y-Intercept Values of Polyimides

	Average Wear Rate (mm^2/kcycle)	95% Confidence Range	Average Y-Intercept (mm^2)	95% Confidence Range
PIA	1.71	1.59 - 1.83	8.55	7.30 - 9.80
PIB	0.56	0.54 - 0.58	5.70	5.46 - 5.92
PIC	1.68	1.50 - 1.86	1.67	-0.28 - 3.63

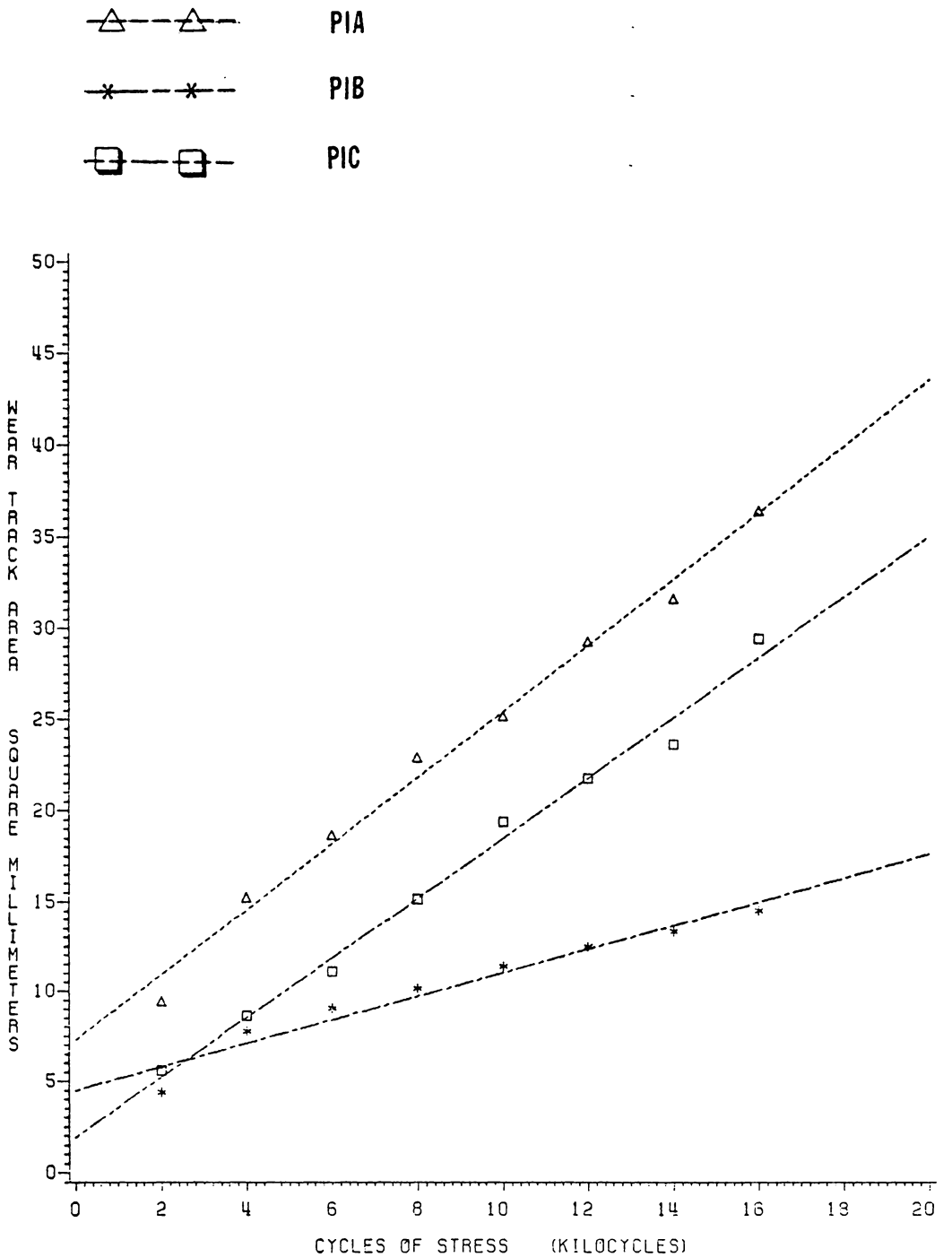

Figure 8: Effect of Structure on Wear

Table 6 Incubation Periods for Polyimides

	Load = 5 N		Load = 10 N	
	Average incubation period (cycles)	95% Confidence range (cycles)	Average incubation period (cycles)	95% Confidence range (cycles)
Speed = 0.63 $\frac{m}{s}$				
PIA	269	90-448	1060	490-1630
PIB	557	355-759	442	221-662
PIC	115	6-224	---	---
Speed = 1.26 $\frac{m}{s}$				
PIC	275	0-611	107	0-239

Table 7 Effect of Sliding Speed on Wear, PIC

Speed (m/s)	Average Wear Rate (mm^2/kcycle)	95% Confidence Range	Average Y-Intercept (mm^2)	95% Confidence Range
0.63	1.68	1.5 - 1.86	1.67	-0.28 - 3.63
1.26	2.30	2.09 - 2.51	14.2	12.1 - 16.3

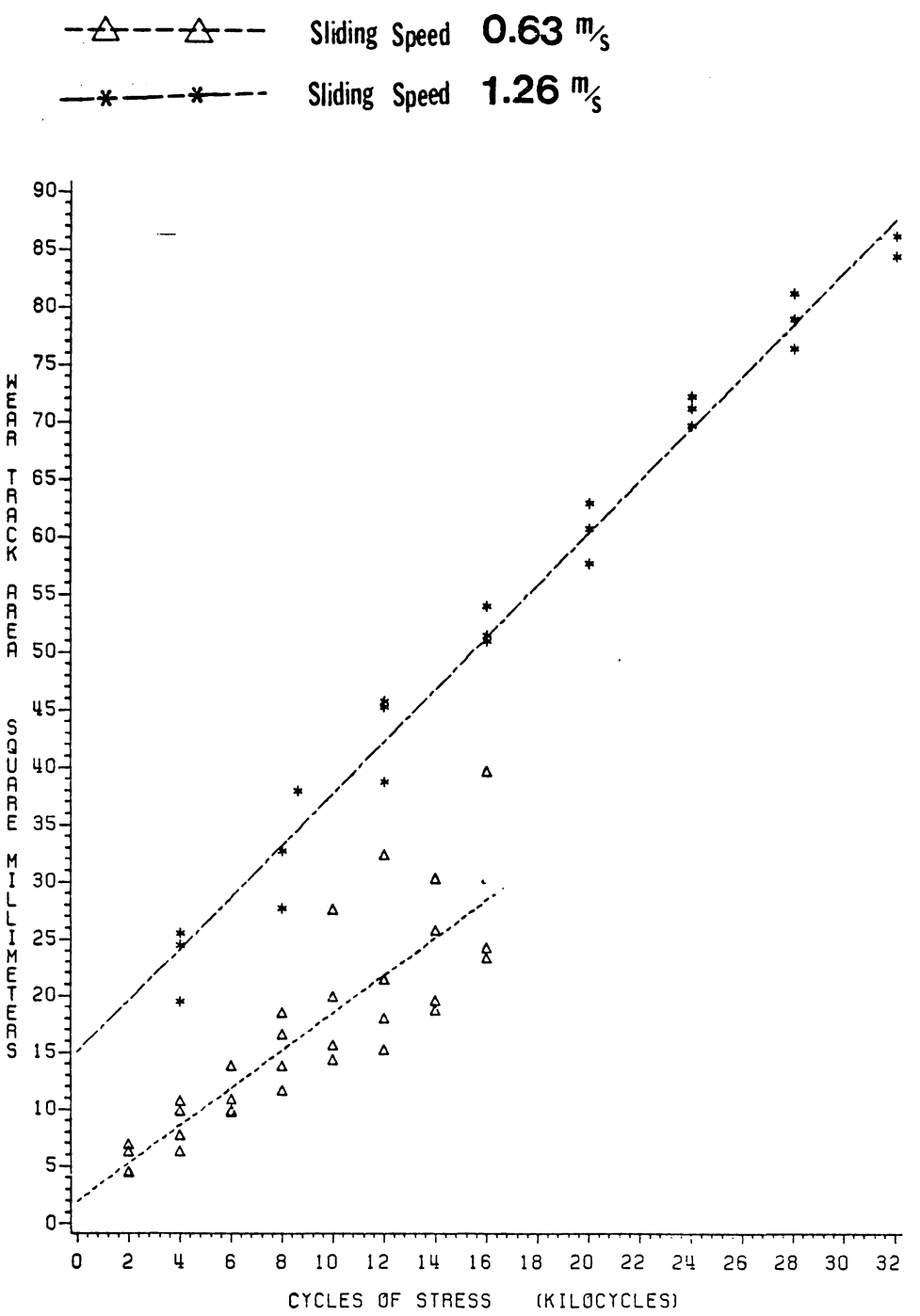

Figure 9: Effect of Sliding Speed on Wear, PIC

B. Friction

The results of the friction testing are summarized in Tables 8 and 9, in which μ_{after} denotes the friction coefficient just after the wear track has fully initiated, μ_{2000} represents the friction coefficient at 2000 cycles, and μ_{16000} represents the friction coefficient at 16000 cycles. The standard deviation, s, and the 95 per cent confidence limits are also presented. For PIB, μ_{after} is not given because PIB underwent a gradual friction transition when the wear track initiated.

At a load of 5 N, PIB exhibited about a 20 per cent lower friction coefficient at 2000 cycles than PIC. The differences between PIB and PIA, and PIA and PIC were statistically insignificant using 95 per cent confidence limits under these conditions. The friction coefficient of PIB at 16000 cycles was 16 per cent lower than PIA and 21 per cent lower than PIC. There were no statistically significant differences between PIA and PIC at 16000 cycles or just after initiation.

At a load of 10 N, both PIA and PIB exhibited lower friction coefficients at 2000 cycles than PIC. The friction coefficient just after initiation was 23 per cent lower for PIA than PIC. The general effect of increasing the load was to decrease the friction coefficient. Doubling the load resulted in a 27 per cent friction coefficient reduction for PIA, a 7 per cent reduction for PIC, and an insignificantly small reduction for PIB.

Figure 10 shows the gradual increase of the friction coefficient with number of cycles for the 16 kilocycle tests. In these tests,

Table 8 Effect of Structure on Friction Coefficient at 5 N Normal Load

	μ_{2000}	95% Confidence Range	s	μ_{16000}	95% Confidence Range	s	μ_{after}	95% Confidence Range	s
PIA	0.26	0.24-0.29	0.03	0.32	0.30-0.33	0.01	0.23	0.21-0.25	0.03
PIB	0.23	0.21-0.26	0.04	0.27	0.26-0.29	0.02	--	---	--
PIC	0.29	0.28-0.31	0.02	0.34	0.31-0.36	0.02	0.24	0.23-0.24	0.01

Table 9 Effect of Structure on Friction Coefficient at 10 N Normal Load

	μ_{2000}	95% Confidence Range	s	μ_{after}	95% Confidence Range	s
PIA	0.19	0.17-0.21	0.02	0.17	0.15-0.19	0.02
PIB	0.23	0.19-0.26	0.03	--	---	--
PIC	0.27	0.26-0.28	0.01	0.22	0.21-0.24	0.02

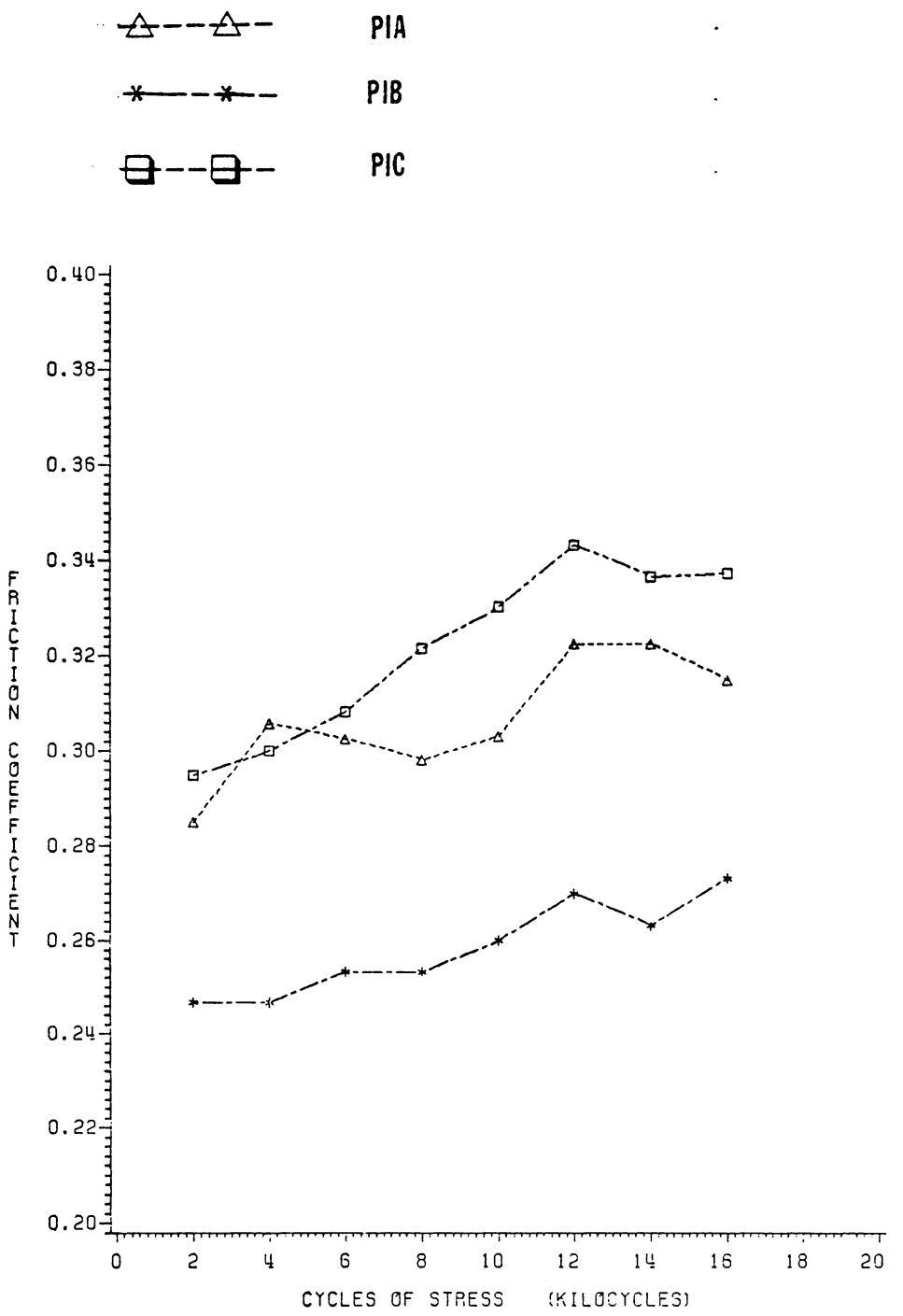

Figure 10: Effect of Structure on Friction

conducted at 5 N loads, the general trend of $\mu_{PIB} < \mu_{PIA} < \mu_{PIC}$ is corroborated. However, the differences between PIA and PIC are usually insignificant.

Figure 11 shows the effect of sliding speed on the friction coefficient of PIC. The basic effect of increasing speed was to increase friction. The scatter in the high speed data was great enough to cause the confidence limits to overlap, however.

C. Scanning Electron Micrographs

Scanning electron microscope photographs were made of the wear tracks to illustrate possible differences in the nature of the wear among the polyimides. The polyimide films which were examined were run for 50,000 cycles at a sliding speed of 0.63 meters per second under a load of 3 N. The wear track of PIC, shown in Fig. 12, suggests that wear occurs by the removal of platelike chunks of material due to friction traction. When the tensile stress induced by friction traction exceeds the rupture energy of the material, a segment of the film at the rear of the contact region may be partially torn away from the surface. During the next pass, the raised lip of the ruptured segment may be fractured to create a wear particle. The ruptured segment and raised lip are shown in Fig. 13 at a high magnification. Of the three tested polyimides, PIC would be most susceptible to this "tearing" type of wear since it has the lowest energy-to-rupture and highest friction coefficients.

Evidence of tearing wear was not detected in the 3 N wear tracks of PIA and PIB (Figs. 14 and 15). Both PIA and PIB exhibit finer wear

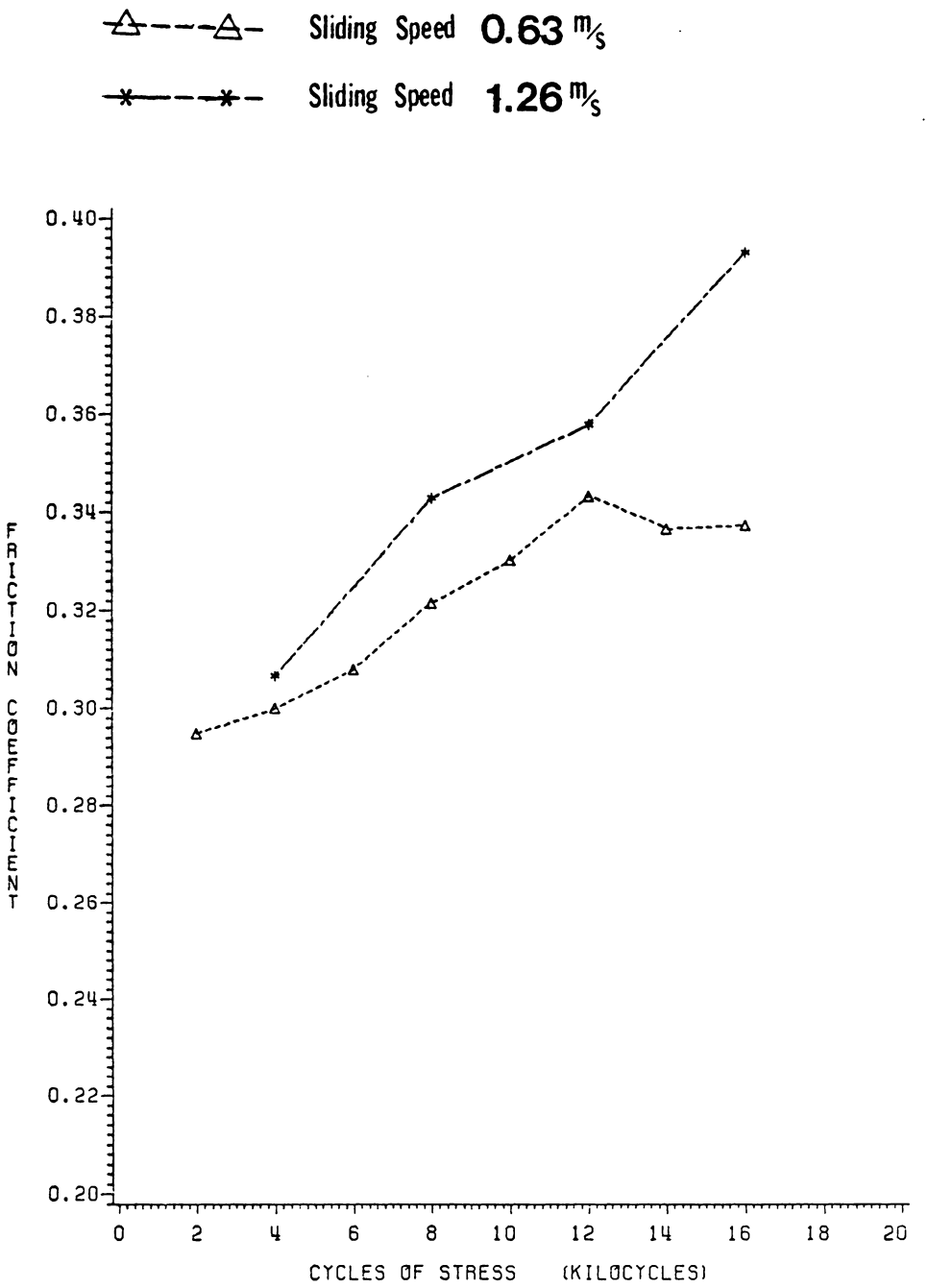

Figure 11: Effect of Sliding Speed on Friction, PIC

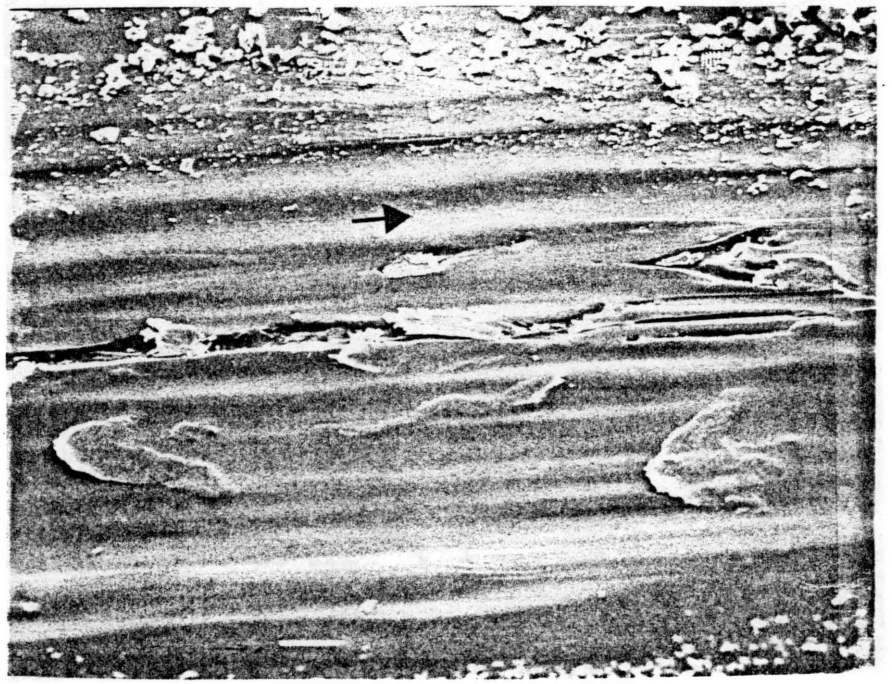

Figure 12: PIC Wear Track, 50000 cycles at 0.63 $\frac{m}{s}$ under 3 N load, arrow indicates direction of sliding, index mark is 50 μm.

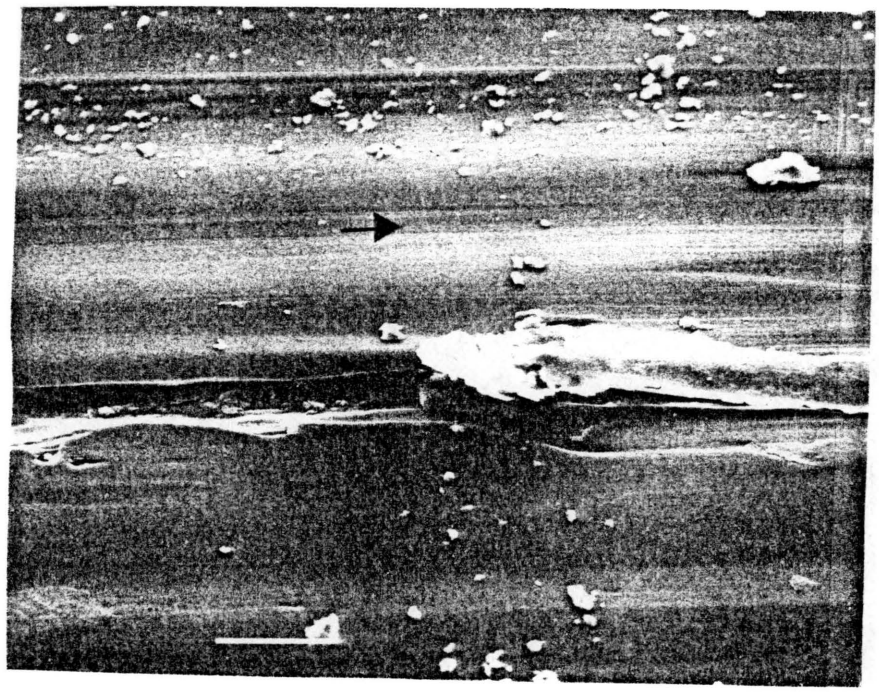

Figure 13: PIC Wear Track, 50000 cycles at 0.63 $\frac{m}{s}$ under 3 N load, arrow indicates direction of sliding, index mark is 50 μm.

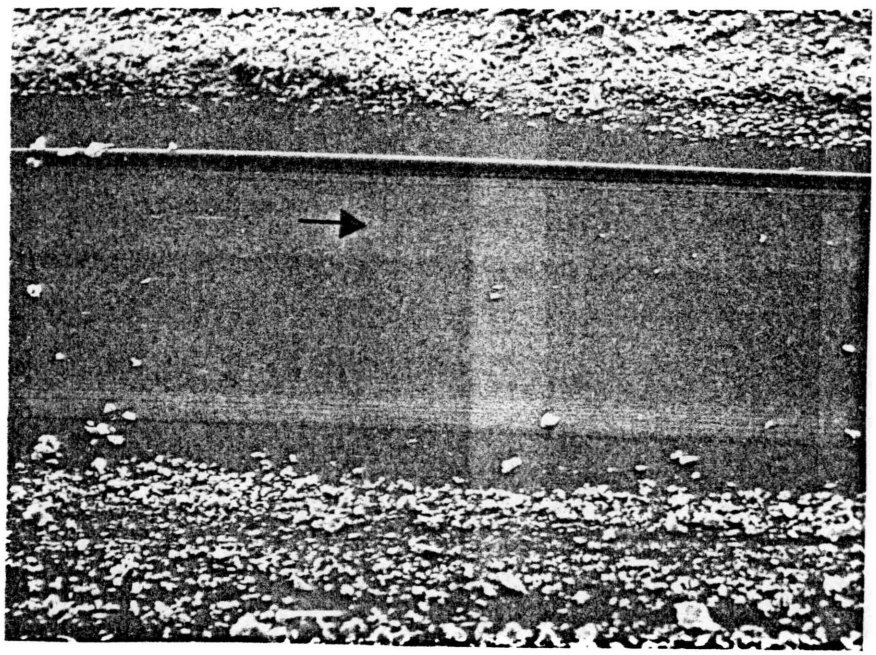

Figure 14: PIA Wear Track, 50000 cycles at 0.64 $\frac{m}{s}$ under 3 N load, arrow indicates direction of sliding, index mark is 50 μm.

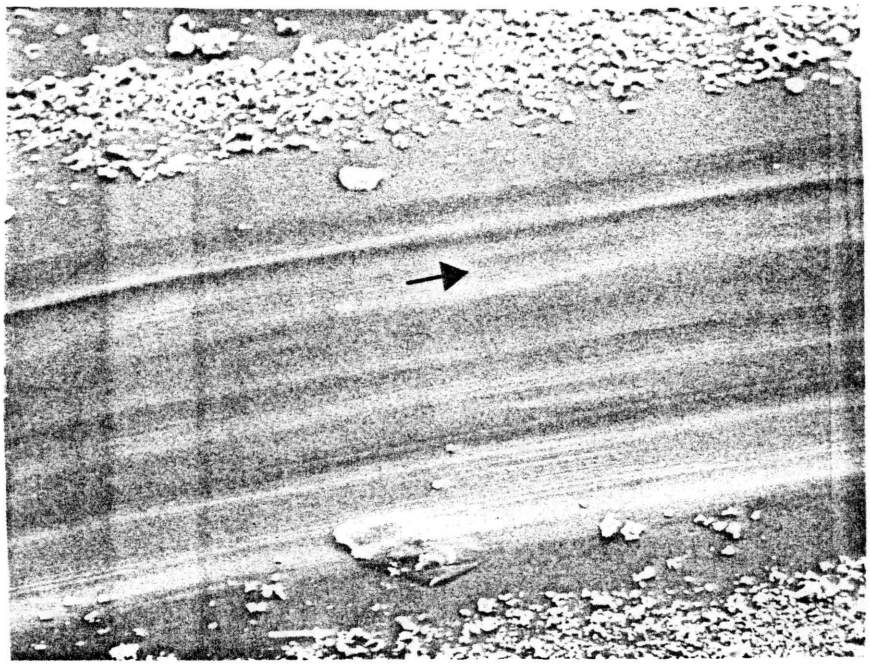

Figure 15: PIB Wear Track, 50000 cycles at 0.63 $\frac{m}{s}$ under 3 N load, arrow indicates direction of sliding, index mark is 50 μm.

debris than PIC. The main difference between PIA and PIB wear tracks seems to be depth, as evidenced by the pronounced edge of the PIA wear track.

DISCUSSION

A. Wear

From test observations and from a process of eliminating other wear modes, the mechanism of wear is proposed to be fatigue. At loads of 5 and 10 N, tests ran up to 2000 cycles with no detectable wear. In preliminary tests at loads of 2 N, samples ran as many as 30,000 cycles without detectable wear. These incubation periods ended with a catastrophic wear track formation distinguished by the generation of wear debris, a sharp increase in friction coefficient, and a temporarily extremely high wear rate. During wear track initiation, the polyimides typically went from no wear track to a wear track with an approximate 2 square millimeter cross-sectional area in a few cycles. No correlation was found between the wear track initiation and the elevation of temperature at the sliding surface. This behavior suggests a fatigue wear mechanism.

Other wear modes seem unlikely. Intuitively the wear mechanism is not abrasive since the tests are conducted with a smooth ball riding on a smooth film. Wear tracks appear smooth in the S.E.M. photographs. If the wear mechanism was adhesive then there is no explanation, other than the presence of a wear inhibiting layer on either ball or film, for the period of no wear. As shown in Table 10, the correlation of the wear data to mechanical properties tends to rule out other wear mechanisms. For an adhesive wear mechanism, higher strength should lead to lower wear, assuming elastic conditions. The experimental results show, however, that higher strength corresponded to high wear. An abrasive

Table 10 Correlation of Wear Rate to Average Mechanical Properties

	Average Wear Rate (mm^2/kcycle)	Ultimate Tensile Strength (MPa)	Elongation to Break (per cent)	Energy to Rupture (MPa)	Elastic Modulus (GPa)
PIA	1.71	113.4	9.2	1042.5	11.94
PIB	0.56	86.0	8.7	749.2	9.74
PIC	1.68	102.9	6.5	684.3	12.39

wear mechanism is also unlikely since there is no correlation between the rupture energy, as approximated by the product of the breaking stress and the elongation to break, and the wear rate.

The correlation of wear data to mechanical properties does suggest a fatigue wear mechanism. The elastic moduli of PIA and PIC, 11.94 and 12.39 GPa respectively, were significantly higher than that of PIB, 9.74 GPa. Correspondingly, the wear rates of PIA and PIC, 1.71 and 1.68 respectively, were significantly higher than that of PIB, 0.56 square millimeters per kilocycle. The fatigue wear model predicts this correlation of wear rate to elastic modulus. According to the fatigue model, the wear rate will be proportional to $(\frac{\sigma}{\sigma_o})^t$, where σ_o is the failure stress corresponding to a single stress application, σ is the applied stress, and t is a material constant [37]. The stress induced in the polymer, as estimated from contact stresses assuming elastic conditions, would be proportional to the elastic modulus, E, to the two-thirds power multiplied by the applied load, P, to the one-third power. Therefore the wear rate assuming a fatigue mechanism is proportional to $P^{t/3}$ $E^{2t/3}$.

Inserting wear results and elastic moduli into the equation

$$W = K\ E^d$$

where W is the wear rate,

K is a constant,

E is the elastic modulus, and

d is a constant,

enables one to calculate values for K and d. The power d was found to be 4.87 and the constant K was found to be 8.62×10^{-6}. The value of d is reasonable since for polymers this parameter varies from approximately 1.3 for ductile materials to approximately 5.3 for brittle materials.

Effect of Structure on Wear Rate

In this section, the polyimides tested are qualified according to the four structural factors mentioned below and each factor is examined for possible correlation to wear rate. The differences in chemical structure which may affect the wear performance of the polyimides are

(1) chain flexibility and freedom of motion allowed by the linking group,

(2) polarity of the linking group, and

(3) regularity of the chain.

Though not directly related to structure, chain length is a wear determining factor which was not controlled in the testing, as evidenced by the different inherent viscosities presented previously in Fig. 3.

The experimental results suggest that, for these polyimides, more flexible systems wear at a lower rate. Of the three polyimides tested, PIB would have the most flexible chain, as indicated by the glass transition temperature because of the presence of the oxygen linking group. Chain rigidity is approximated by the glass transition temperature since chains with less internal mobility inhibit the glass transition by storing thermal energy through steric hindrance [1]. The oxygen linking group allows a great deal of chain movement and can have a marked effect on the bulk rigidity of a polyimide. For example a

certain aromatic polyimide which contains the linking group A shown in Fig. 16 has an elongation to failure of 2 per cent, while the same polyimide with the more flexible linking group B has an elongation to failure of 80 per cent. The same polyimide with the even more flexible group C has a elongation to failure of 120 per cent [8]. Correspondingly, PIB, the polyimide polymerized from the diamine with the flexible oxygen linkage, had the lowest wear rate.

Of the two remaining polyimides, PIC would have the less flexible chains due to its greater density of double bonds and highly polar carbonyl groups. The chain is stabilized by a double bond because the pi orbital bond restricts the movement of neighboring atoms and hence increases chain rigidity. A high density of polar groups increases chain rigidity due to the repulsion of like charges. Despite this, the glass transition temperature of PIA is slightly high than that of PIC. This is probably due to PIA's increased molecular weight and correspondingly longer average chain length as indicated by the significantly larger inherent viscosity.

If one accepts glass transition temperature as a measure of chain rigidity, then there is a good correlation between chain rigidity and wear rate. This correlation is presented in Table 11.

In addition to their effect on chain flexibility, highly polar side groups may have a direct effect on wear rate. In crystalline and semi-crystalline systems, the presence of highly polar side groups would tend to lead to lower wear by inducing a higher degree of crystallinity, thereby inhibiting crack propagation. In crystalline polymers, crack propagation involves the breaking of primary bonds because the polymer

Elongation to failure of a certain polyimide containing this linkage

A 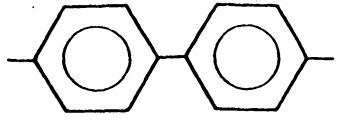

2 %

B 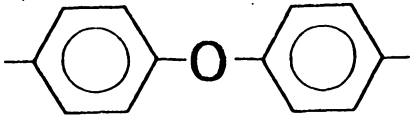

80 %

C 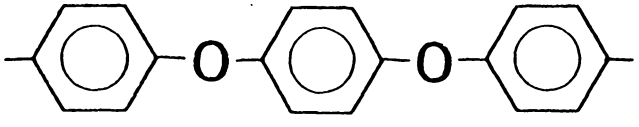

120 %

Figure 16: The effect of the Flexible Oxygen Linkage on Rigidity

Table 11 Correlation of Wear Rate to Chain Rigidity, as Approximated by Glass Transition Temperature

	Wear Rate (mm^2/kcycle)	Glass Transition Temperature (°C)
PIA	1.71	295
PIB	0.56	257
PIC	1.68	288

chains cannot reorient to allow slippage [38]. For predominantly amorphous systems, the increased tendency toward some degree of crystallinity has much less effect on crack propagation, since cracks may easily propagate through the amorphous regions. Therefore, for the primarily amorphous polyimides tested, the wear inhibiting effects of polarity-induced crystallinity are greatly diminished since wear properties are dominated by the amorphous regions.

Highly polar side groups could conceivably lead to increased interaction and adhesion to the contacting model or transferred film. Increased adhesion would lead to higher tractive stresses and correspondingly higher wear rates. The S.E.M. photographs support this hypothesis since PIC, with the highly polar carbonyl group, was the only polyimide to exhibit signs of gross transfer.

The effect of the structure on chain regularity may also play some role in determining wear. Of the three polyimides, PIC would have the most regular chain because the PIC diamines, containing carbonyl linkages, are more similar to the common dianhydride than the PIA and PIB diamines are. A structural unit that would tend to increase regularity would tend to produce a less elastic, more rigid polymer [11]. It is hypothesized that, for fatigue wear, this change in properties would lead to a higher wear rate. However, like the polarity effect, increased regularity is believed to play a much smaller role in determining wear for amorphous polymers relative to crystalline polymers.

Though not directly related to structure, the chain length, as approximated by molecular weight, may have affected the wear rates of the polyimides. Longer polymer chains in high molecular weight

materials lead to higher mechanical properties and tend to decrease wear since they more likely require primary bond breakage for crack propagation [38]. Possibly molecular weight did play a significant role in determining wear performance as suggested by the decreased wear rate for PIB, the polyimide with the highest molecular weight. However, molecular weight was obviously not the dominant factor as evidenced by the similar wear performance of PIA and PIC despite the relatively large difference in their molecular weights.

Fusaro tested two condensation type polyimides whose tribological performance may have been affected by some of the previously mentioned factors. Fusaro's PIC-7, analogous to PIC, had a high density of highly polar carbonyl groups, while his PIC-6 had a number of oxygen linkages making it analogous to PIB. In tests conducted at 25°C, Fusaro observed a wear rate for PIC-7 three times higher than that of PIC-6 [25].

Effect of Sliding Speed on Wear Rate

Increasing the sliding speed produces two effects: an increase in the rate at which the polymer is strained and an increase in the temperature at the metal-polymer interface. The increase in strain rate should lead to a decrease in the polymer's ability to yield without failing. The corresponding increase in the elastic modulus should lead to higher wear, since the increase in strain rate would give the polyimide chains less time to reorient and relieve stress. Consequently, bonds in the main chain would be broken more frequently. The effect of increased temperature would tend to counterbalance the effect of strain rate by slightly lowering the elastic modulus.

B. Friction

The friction force generated between two surfaces in relative motion is generally accepted to be made up of two components--the adhesive force and the deformation force. For polymers, both terms are usually significant [39]. However, in this testing the adhesive component is emphasized, since the contact geometry was a smooth ball riding on a smooth film. Therefore, PIB's relatively low friction coefficient can be explained by noting its lower shear strength and extrapolating that consequently less force would be required to shear the junctions at its real area of contact.

The other factor which would affect the adhesive component of friction would be the real area of contact. The effect on friction of the real area of contact would partially counterbalance the effect of lower shear strength. For a ball on flat configuration under elastic conditions, PIB would have the largest real area of contact. Contact area equations are presented in Appendix D. Since PIA and PIC would have virtually the same areas of contact, the difference in their shear stress would suggest slightly higher adhesive friction components for PIA. Other factors are needed to explain PIC's higher friction.

In virtually all tests, the friction coefficient increased slightly as the number of cycles increased. Calculations were made to determine whether the growth of the real contact area, as extrapolated from the dimensions of the wear track, would explain this friction increase. As shown in Table 12 there is an increase in the real contact area for all the polyimides except PIC, which exhibited a slight decrease. Since

Table 12 Calculated Real Contact Areas

	Contact Area (m^2)		
	Initial (Ball on Flat)	2 kcycles (Ball in Groove)	16 kcycles (Ball in Groove)
PIA	1.819×10^{-8}	2.134×10^{-8}	2.425×10^{-8}
PIB	2.066×10^{-8}	3.150×10^{-8}	3.307×10^{-8}
PIC	1.777×10^{-8}	2.333×10^{-8}	2.285×10^{-8}
PIC (double speed)	1.777×10^{-8}	2.297×10^{-8}	2.640×10^{-8}

PIC's friction coefficient increased with number of cycles, the change in real contact area does not account for the friction change. No correlation was noted between fluctuations in friction coefficient and real contact area. However, the real contact area calculations are based on the size of the wear track and do not include the effect of thermal softening. The build-up of heat and consequent decrease in elastic modulus would tend to increase the real contact area. As shown in Table 12 the change in real contact area does account for the friction change which accompanies wear track initiation.

The importance of the deformation component of friction is suggested by the correlation of rougher than normal wear tracks with high friction. The wear tracks of all these polyimides are relatively smooth and featureless, except that PIC tracks exhibit an occasional pit or hole. However, some wear tracks of each polyimide appear very slightly rougher than others of the same polyimide. Test results indicate some correlation between wear track roughness and higher friction. For example, for PIC tested at a radius of 1.66 cm, a rougher than normal wear track, noted at 2 kilocycles, coincided with a measured friction coefficient which was almost 2 standard deviations greater than the mean friction. As shown in Table 13, of the 19 roughest wear tracks, 74 per cent had above average friction coefficients, and 26 per cent had below average friction coefficients. The 14 wear tracks which exhibited higher friction had friction coefficients which, on the average, were 0.84 standard deviations above the norm. Four of the tracks coincided with friction coefficients which were above the 95 per cent confidence limits. Of the five PIC wear tracks which contained a pit, four had

Table 13 Correlation of Friction Coefficient to Wear Track Roughness

Polyimide	Kilocycles	Observed Friction Coefficient	Average Friction Coefficient	Number of Stnd. Dev. from Mean
PIA	2	0.25	0.26	− 0.4
	4	0.31	0.31	+ 0.3
	6	0.31	0.30	+ 1.0
	8	0.33	0.30	+ 1.5
	10	0.30	0.31	− 1.0
	12	0.36	0.32	+ 1.3
	14	0.37	0.32	+ 1.7
PIB	2	0.25	0.23	+ 0.6
	4	0.23	0.25	− 1.0
	6	0.23	0.25	− 1.0
PIC	2	0.30	0.29	+ 0.2
	2	0.33	0.29	+ 1.8
	*4	0.31	0.30	+ 0.3
	*6	0.32	0.31	+ 0.2
	6	0.34	0.31	+ 0.8
	*8	0.32	0.32	− 0.2
	8	0.34	0.32	+ 1.0
	*12	0.36	0.34	+ 1.0
	*16	0.34	0.34	+ 0.1

* Denotes Pitted Wear Track

above average friction coefficients and one had a below average friction coefficient. Overall, the increased roughness of the PIC wear tracks partially explains PIC's higher friction coefficient.

The wear tracks produced during the PIC double speed testing are not mentioned in Table 13 because none showed any appreciable roughness on pitting. The smoothness of the double speed wear tracks may be partially due to the increased temperature generated at the elevated speed. As measured by a thermocouple placed near the wear track surface, the steady state temperature ranged from 40 to 45°C during double speed testing and from 33 to 38°C during normal speed testing. The increased heat energy generated at the higher speed may have allowed the wear particles to form in a more ductile manner leading to a smoother wear track.

Two partially counterbalancing effects, increased strain rate and increased temperature, influenced the friction of the high speed tests. The increased strain rate would tend to increase the elastic modulus, resulting in a smaller contact area and a corresponding decrease in friction. The increased temperature would have the opposite effect on elastic modulus, leading to a larger contact area and an increase in friction. Judging from friction results and contact area calculations, the thermal effect apparently affected friction more than the strain rate effect.

Polarity may explain the higher friction for PIC. Belyi [40] found that extremely high friction resulted when rubbing highly polar polymers such as polymethylmethacrylate and polycaproamide. He attributed the

high friction directly to the polar nature of the polymers. Belyi [41] also reports that as film thickness decreases, the friction coefficient increases. Since PIC had the thinnest film, a slight increase in its friction coefficient may have been noted.

CONCLUSIONS

The wear mechanism was proposed to be fatigue since the polyimide experienced an incubation period followed by the catastropic initiation of a wear track. The initiation of the wear track was distinguished by the generation of wear debris, a sharp increase in friction coefficent, and an extremely high wear rate. The fatigue mechanism is also suggested by the correlation of wear rate with elastic modulus. There was no correlation between the energy-to-rupture parameter, sE, and wear rate.

A correlation between chain flexibility and wear rate was noted. The more flexible the chain, as approximated by the glass transition temperature, the lower the wear rate. S.E.M. photographs and pitted wear tracks suggested that the presence of highly polar side groups led to higher wear for PIC. Molecular weight, or chain length, was not a dominant wear determining factor. For PIC, doubling the sliding speed increased the wear rate (per cycle) by 37 per cent.

A correlation was observed between low shear strength and low friction. This is attributed to the predominance of the adhesion component of friction for a smooth ball riding on a smooth film. The growth of the real area of contact explains the friction increase during wear track initiation. However, the growth of the real area of contact does not explain the slight friction increase with number of cycles, unless thermal softening causes greater area growth than calculated. The importance of the deformation component of friction is suggested by the correlation of wear track roughness to high friction. Increased rough-

ness, increased polarity, and smaller film thickness contributed to PIC's highest friction coefficient. For PIC, increasing the sliding speed led to higher friction.

RECOMMENDATIONS

1. Tests at higher shear rates (higher sliding velocities) should be conducted on PIB and PIC to isolate the effect of chain flexibility on friction and wear properties. As the shear rate is increased, the tribological performance of PIB should approach that of PIC if chain flexibility is an important friction-and-wear-determining factor.
2. More work is needed to characterize the wear track initiation. S.E.M. examination of a wear track which is undergoing wear track initiation may be instructive.
3. More work is needed to characterize the incubation period. The effect of different test procedures could be investigated by comparing incubation periods for non-stop testing to testing which is halted after each 100 cycles.
4. A reliable method of monitoring temperature at, or close to, the sliding interface should be incorporated into future testing.
5. The effect of molecular weight should be investigated by obtaining PIC with an inherent viscosity closer to PIA or PIB.

REFERENCES

1. Rosen, S. L., Fundamental Principles of Polymeric Materials, John Wiley & Sons, New York, 1982.

2. Fusaro, R. L., "Tribological Properties and Thermal Stability of Various Types of Polyimide Films," NASA-TM-81765, 1981.

3. Fusaro, R. L., "Friction and Wear Life Properties of Polyimide Thin Films," NASA-TN-D-6914, 1972.

4. Fusaro, R. L., "Friction Transition in Polyimide Films as Related to Molecular Relaxations and Structure," NASA-TN-D-7954, 1975.

5. Carter, J. T., "An Investigation of Polymer Wear Due to Fatigue Using a Constant Strain Wear Test," Master's Thesis, Virginia Polytechnic Institute and State University, 1983.

6. Bower, G. M., L. W. Frost, "Aromatic Polyimides," Journal of Polymer Science, pt. A, Vol. 1, No. 10, 1963, pp. 3135-3150.

7. Rodriguez, F., Principles of Polymer Systems, McGraw-Hill, New York, 1970.

8. Koton, M. M., "Mechanical Properties, Thermal Stability, and Synthesis of Aromatic Polyimides, Amide-Imides, Ester-Imides, and Pyrrones," RAE-LIB-TRANS-1499, N71-19631, Oct. 1970.

9. Todd, N. W., and F. A. Wolff, "Polyimide Plastics Withstand High Temperatures," Materials in Design Engineering, Vol. 60, No. 2, Aug. 1964, pp. 86-91.

10. Gilham, J. K., and H. C. Gilham, "Polyimides: Effect of Molecular Structure and Cure on Thermomechanical Behavior," Polymer Engineering Science, Vol. 13, No. 6, Nov. 1973, pp. 447-454.

11. Prokopchuk, N. R., Y. Baklagina, L. Korzhavin, A. Sidorovich, M. Koton, "Effect of Molecular Orientation and Crystallization and Cure on Thermomechanical Behavior," Polymer Engineering Science USSR, Vol. 19, No. 5, 1977, pp. 1297-1304.

12. Wallach, M. L., "Structure Property Relations of Polyimide Films," American Chemical Society - Division of Polymer Chemistry, Vol. 8, No. 1, 1967, pp. 656-663.

13. Cassidy, P. E., Thermally Stable Polymers, Marcell Dekker, New York, 1980.

14. Hergenrother, P. N., NASA Langley, American Chemical Society Short Course Notes.

15. Sroog, C. E., "Polyimides," Journal of Polymer Science - Polymer Symposia, Pt. C, No. 16, Pt. 2, 1967, pp. 1191-1209.

16. Varma, I. K., R. N. Goel, D. S. Varma, "Effect of Structure on the Thermal Stability of Polyimides," Journal of Polymer Science: Polymer Chemistry Edition, Vol. 17, No. 3, March 1979, pp. 703-713.

17. Butta, E., S. DePetris, M. Pasquini, "Young's Modulus and Secondary Mechanical Dispersions in Polypyromellitimide," Journal of Applied Polymer Science, Vol. 13, No. 6, June 1969, pp. 1073-1081.

18. Ikeda, R. M., "A Mechanical Effect of Orientation," American Chemical Society - Division of Polymer Chemistry, Polymer Preprints, Vol. 6, No. 2, Sept. 1965, pp. 807-830.

19. Bernier, G. A., D. E. Kline, "Dynamic Mechanical Behavior of a Polyimide," Journal of Applied Polymer Science, Vol. 12, No. 3, March 1968, pp. 593-604.

20. Lim, T., V. Frosini, V. Zaleckas, D. Morrow, J. Saver, "Mechanical Relaxation Phenomena in Polyimide and Poly (2,6-dimethyl p-phenylene oxide) from 100° to 700°K," Polymer Engr. Sci., Vol. 13, No. 1, Jan. 1973, pp. 51-58.

21. Fusaro, R. L., "Effect of Atmosphere and Temperature on Wear, Friction, and Transfer of Polyimide Films," Trans. ASLE, Vol. 21, No. 2, April 1978, pp. 125-133.

22. Fusaro, R. L., "Polyimide Film Wear-Effect of Temperature and Atmosphere," NSAS-TN-D-8231, 1976.

23. Fusaro, R. L., "Molecular Relaxations, Molecular Orientation, and the Friction Characteristics of Polyimide Films," Trans. ASLE, Vol. 20, No. 1, Jan. 1977, pp. 1-14.

24. Fusaro, R. L., "Effect of Thermal Exposure on Lubricating Properties of Polyimide Films and Polyimide-Bonded Graphite Fluoride Films," NASA-TP-1125, 1978.

25. Fusaro, R. L., "Comparison of the Tribological Properties at 25°C of Seven Different Polyimide Films Bonded to 301 Stainless Steel," NASA-TM-81413, 1980.

26. Fusaro, R. L., "Lubrication and Wear Mechanisms of Polyimide-Bonded Graphite Fluoride Films Subjected to Low Contact Stress," NASA-TP-1584, 1980.

27. Giltrow, J. P., "Friction and Wear of Some Polyimides," Tribology (London), Vol. 6, No. 6, Dec. 1973, pp. 253-257.

28. Salomon, G., Discussion of Fusaro, R. L., "Molecular Relaxations, Molecular Orientation, and the Friction Characteristics of Polyimide Films," Trans. ASLE, Vol. 20, No. 1, Jan. 1977, pp. 1-14.

29. Bill, R. C., "Fretting of AISI 9310 Steel and Selected Fretting-Resistant Surface Treatments," ASLE Trans., Vol. 21, No. 3, July 1978, pp. 236-242.

30. Buckley, D. H., and R. L. Johnson, "Degradation of Polymeric Compositions in Vacuum to 10^{-9} mm Hg in Evaporation and Sliding Friction Experiments," Soc. Plastics Engrs. Trans., Vol. 4, No. 4, Oct. 1964, pp. 306-314.

31. Buckley, D. H., "Friction and Wear Characteristics of Polyimide and Filled Polyimide Compositions in Vacumm," NASA-TN-D-3261, 1966.

32. Devine, M. J., and A. E. Kroll, "Aromatic Polyimide Compositions for Solid Lubrication," Lubr. Eng., Vol. 20, No. 6, June 1964, pp. 225-230.

33. Gardos, M. N., and B. D. McConnell, "Development of a High Load, High Temperature, Self-Lubricating Composite," Paper presented at 1981 ASLE-ASME Lubrication Conference, October 5-7, 1981, New Orleans, LA.

34. Jones, W. R., W. F. Hady, and R. L. Johnson, "Friction and Wear of Poly(Amide-Imide), Polyimide, and Pyrrone Polymers at 260°C (500°F) in Dry Air," NASA-TN-D-6353, 1971.

35. Prikhodko, O. G., et al., "Mechanical Properties of Amorphous and Crystalline Fenilons," Soviet Plastics, No. 7, 1969, pp. 53-55.

36. Eiss, N. S., Jr., and S. C. Milloy, "The Effect of Asperity Curvature on Polymer Wear," Wear of Materials 1983, ed. Ludema, K. C., ASME, New York, NY, 1983, pp. 650-656.

37. Lancaster, J. K., "Basic Mechanisms of Friction and Wear of Polymers," Plastics and Polymers, Vol. 41, Dec. 1973, pp. 297-305.

38. Sauer, J. A., E. Foden, D. R. Morrow, Polymer Engineering Science, Vol. 17, 1977, p. 246.

39. Eiss, N. S., "The Influence of Surface Topography on Polymer Friction," Proceedings of International Conference on Tribology in the 80's, NASA Lewis Research Center, 1983.

40. Belyi, V., V. Savkin, A. Sviridyonok, "Role of Structure in Friction Mechanisms of Polymer Materials," Advances in Polymer Friction and Wear, Plenum Press, New York, 1974.

41. Belyi, V., V. Savkin, A. Sviridyonok, V. Smurugov, O. Kholodilov, "An Investigation of Molecular Mobility in Polymers Under Rubbing Contact," Wear, Vol. 42, 1977, pp. 91-97.

42. Timoshenko, S., and J. N. Goodier, Theory of Elasticity, McGraw-Hill, New York, 1951.

APPENDIX A

Film Casting and Curing Procedure

The polymerization reaction by which the tested polyimides were produced is shown in Fig. 17. The supplied polyamic acids were dissolved in N,N - dimethylacetamide (DMAC) at a concentration of approximately 15 per cent weight of polymer per volume of solvent (w/v).

Before film spreading, the substrates, shown in Fig. 6 were cleaned with soap and water, with acetone, and then with DMAC. The doctor's blade was washed with DMAC before spreading. The solutions were spread using the .030" side of the doctor's blade onto type 410 stainless steel substrates. The substrates had been surface ground to the surface characterization parameters shown in Table 14.

After spreading, the films were allowed to air dry for 24 hours, with provisions taken to prevent dust or contaminant particles from meeting the film surface. The the films were cured by heating at 70°C for 1 hour, 140°C for 1 hour, and 200°C for 1 hour.

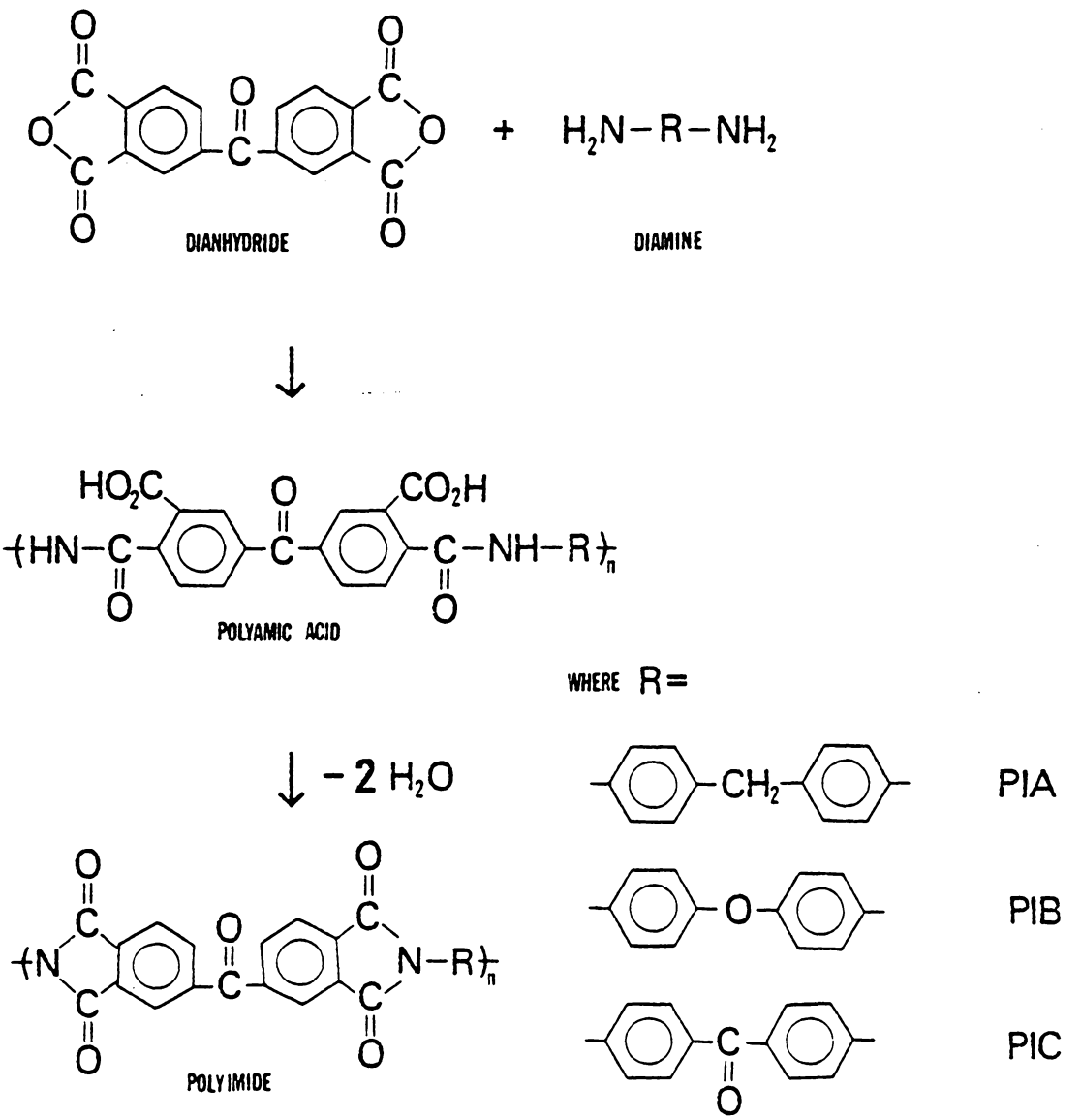

Figure 17: Polymerization Reaction for Tested Polyimides

Table 14 Surface Parameters for Steel Substrates

CMS DATA FILE I.D. (FN/FT/FM)		RA ROUGH. ALSO CLA (microns)	MEAN SQUARE DEVIATION (microns sq)	(RMS) (um)	SKEWNESS (nondim.)	KURTOSIS (nondim.)	MAX PEAK TO VALLEY (microns)
1) JJSUB1	>	1.0678	1.7315	(1.3159)	-0.114	2.664	7.1774
2) JJSUB2	>	1.2285	2.6166	(1.6176)	-0.852	4.485	10.0908
3) JJSUB3	>	1.3821	3.2784	(1.8106)	-0.481	3.837	11.7148
4) JJSUB4	>	1.1809	2.3545	(1.5344)	-0.651	3.906	9.4397
5) JJSUB5	>	1.1922	2.2288	(1.4929)	-0.269	3.245	9.0738
6) JJSUB6	>	1.2879	2.7390	(1.6550)	-0.069	3.170	9.5009
7) JJSUB7	>	1.4731	3.8227	(1.9552)	-0.460	4.417	14.3215
8) JJSUB8	>	1.4015	3.2126	(1.7924)	-0.595	3.538	10.3398
9) JJSUB9	>	1.2154	2.4964	(1.5800)	-0.350	4.116	11.2094
10) JJSUB10	>	1.1484	2.5837	(1.6074)	-1.353	6.294	10.8238
AVERAGE	>	1.2578	2.7064	(1.6361)	-0.519	3.967	10.3692
STD.DEV.	>	0.1266	0.5963	(0.1810)	0.379	0.998	1.8829

APPENDIX B

Polymer Mechanical Properties

A set of films were cast and cured on glass, removed, and cut into tensile specimens. The specimens were then pulled to break in an Instron tension tester. The mechanical properties were obtained from the load-elongation curves as follows:

1. Ultimate Tensile Strength - the load at break divided by original cross-sectional area of the specimen.
2. Elongation to Break - the elongation at break divided by the original specimen length.
3. Energy to Rupture Parameter - the product of the ultimate tensile strength and the elongation to break.
4. Modulus of Elasticity - the initial slope of the load-elongation curve multiplied by the original specimen length and divided by the original specimen cross-sectional area.

Table 15 Film Mechanical Properties

95 per cent confidence range is given in parenthesis

	Ultimate Tensile Strength (MPa)	Elongation to Break (per cent)	Modulus of Elasticity (GPa)	Energy to Rupture Parameter (MPa)
PIA	113.4	9.2	11.94	1042.5
	(97.3-129.5)	(6.8-11.5)	(9.86.14-01)	(754.2-1330.9)
PIB	86.0	8.7	9.74	749.2
	(80.4-91.5)	(6.9-10.4)	(9.02-10.46)	(568.4-929.9)
PIC	102.9	6.5	12.39	684.3
	(87.7-118.0)	(5.3-7.7)	(10.79-13.99)	(454.8-913.8)

APPENDIX C

Table 16 Wear Data, PIA

Wear Track Cross-sectional Area
(mm^2)

	Wear Track Radius (cm)			
kc	1.13	1.34	1.66	1.13
2	9.000	9.750	8.000	11.10
4	16.250	13.00	13.25	18.625
6	20.000	16.00	16.50	22.325
8	23.000	22.25	20.50	26.050
10	25.25	23.25	22.75	29.550
12	31.75	28.25	25.00	32.325
14	35.25	29.00	28.00	34.250
16	39.75	36.00	33.25	36.825

Table 17 Wear Data, PIB

Wear Track Cross-Sectional Area
(mm^2)

	Wear Track Radius (cm)			
kc	1.13	1.34	1.50	1.66
2	--	4.750	4.800	3.700
4	12.000	6.025	7.200	5.925
6	13.000	7.325	8.500	7.375
8	13.500	9.050	9.750	8.450
10	14.500	10.125	11.300	9.650
12	16.250	11.200	11.500	11.050
14	16.250	12.375	12.850	11.950
16	17.750	13.200	13.400	13.775

Table 18 Wear Data, PIC

Wear Track Cross-Sectional Area
(mm^2)

Sliding Speed = 0.63 $\frac{m}{s}$

	Wear Track Radius (cm)			
Kc	1.13	1.34	1.50	1.66
2	6.325	6.975	4.550	4.475
4	10.750	9.875	7.700	6.275
6	13.875	10.900	9.925	9.825
8	16.600	18.500	13.875	11.700
10	19.925	27.675	15.650	14.425
12	21.450	32.450	18.025	15.275
14	25.825	30.325	19.625	18.800
16	30.325	39.700	23.450	24.300

Sliding Speed = 1.26 $\frac{m}{s}$

	Wear Track Radius (cm)		
Kc	1.13	1.34	1.66
4	25.50	24.50	19.50
8	32.75	38.00	27.75
12	45.25	45.75	38.75
16	51.50	54.00	51.00
20	63.00	60.75	57.75
24	69.75	71.25	72.25
28	81.25	76.50	79.00
32	86.25	84.50	86.25

APPENDIX D

Contact Area Equations

The contact area for a ball on a flat was estimated using Hertzian Contact Theory [42]. The area of contact, AR, was calculated to be

$$AR = \pi a^2 \tag{1}$$

where a is given by equation 3. The contact area for a ball in a groove, AG, was also estimated using Hertzian Contact Theory. The area is given by equation 2 below.

$$AG = \pi ab \tag{2}$$

$$a = m \left[\frac{3\pi F}{4} \frac{K_1 + K_2}{A + B} \right]^{1/3} \tag{3}$$

$$b = a \frac{n}{m} \tag{4}$$

$$K_1 = \frac{(1 - \mu_1^2)}{\pi E_1} \tag{5}$$

$$K_2 = \frac{(1 - \mu_2^2)}{\pi E_2} \tag{6}$$

$$m,n = f(\cos\theta) \quad \text{given in reference 42} \tag{7}$$

$$\cos\theta = \frac{B - A}{A + B} \tag{8}$$

$$A + B = \frac{2}{D_1} + \frac{1}{D_2} \tag{9}$$

$$B - A = \left| \frac{1}{D_2} \right| \tag{10}$$

where

D_1 = diameter of the ball

D_2 = negative of the diameter of the groove

F = applied normal force

μ_1 = poisson's ratio for the ball material

μ_2 = possson's ratio for the film material

E_1 = elastic modulus for the ball material

E_2 = elastic modulus for the film material

The vita has been removed from the scanned document